RESEARCH PAPER

Reliability-based robust design optimization using the eigenvector dimension reduction (EDR) method

Byeng D. Youn · Zhimin Xi

Abstract This paper presents an effective methodology for reliability-based robust design optimization (RBRDO). The eigenvector dimension reduction (EDR) method plays a pivotal role in making RBRDO effective because the EDR method turns out to be very efficient and accurate for probability analysis. The use of the EDR method provides three benefits to RBRDO. First, an approximate response surface facilitates sensitivity calculation of reliability and quality where the response surface is constructed using the eigenvector samples. Thus, sensitivity analysis becomes very efficient and simple. Second, one EDR execution evaluates a set of quality (objective) and reliability (constraint) functions. In general, the EDR requires $2N + 1$ or $4N + 1$ simulation runs where N is the total number of random variables. The EDR execution does not require an iterative process, so the proposed RBRDO methodology has a single-loop structure. Moreover, the EDR execution time can be much shorter by taking advantage of a parallel computing power, and RBRDO can be far more efficient. Third, the EDR method allows solving problems with statistically correlated and non-normally distributed random inputs. Three practical engineering problems are used to demonstrate the effectiveness of the proposed RBRDO method using the EDR method.

B. D. Youn (✉) · Z. Xi
Department of Mechanical Engineering,
University of Maryland, College Park,
MD 20742, USA
e-mail: bdyoun@umd.edu

1 Introduction

Probability analysis is an essential tool to observe the effect of uncertainty (e.g., manufacturing variability and loads) in engineering systems. However, a common challenge in probability analysis is a multidimensional integration to quantify the probabilistic nature of the system responses. It is almost impossible to conduct the multidimensional integration analytically and numerically. Other than direct integration approach, the existing approximation methods for probability analysis can be categorized into four groups: (1) sampling method; (2) expansion method; (3) the most probable point (MPP)-based method; and (4) approximate integration method.

The sampling method is most comprehensive but expensive for estimating statistical moments, reliability, and quality of system responses. Monte Carlo simulation (MCS; Varghese et al. 1996; Lin et al. 1997) is the most widely used sampling method but demands thousands of computational analyses [e.g., finite element analysis (FEA), crash analysis, etc.]. To relieve the computational burden, other sampling methods have been developed, such as quasi-MCS (Niederreiter and Spanier 2000; Sobol 1998), (adaptive) importance sampling (Engelund and Rackwitz 1993; Melchers 1989; Bucher 1988; Wu 1994), directional sampling (Bjerager 1988), etc. Nevertheless, sampling methods are considerably expensive but accurate with a sufficiently large

size of samples. Hence, it is often used for the verification of probability analysis when alternative methods are employed.

The idea of the expansion method is to estimate the statistical moments of system responses with a small perturbation to simulate the input uncertainty. This expansion method includes Taylor expansion (Jung and Lee 2002), perturbation method (Kleiber and Hien 1992; Rahman and Rao 2001), the Neumann expansion method (Yamazaki and Shinozuka 1988), etc. The expansion methods could become computationally inefficient or inaccurate when the degree of input uncertainty is high. Moreover, as it requires high-order partial sensitivities of system responses to maintain good accuracy, it may not be practical for large-scale engineering applications.

The MPP-based method has been widely used to perform reliability analysis. Rotationally invariant reliability index is introduced through a nonhomogeneous transformation (Hasofer and Lind 1974). Probability analysis can be conducted in two different ways: performance level (G-level; Hasofer and Lind 1974) and probability level (P-level; Youn et al. 2004a; Du and Chen 2002) methods. It has been found that the P-level method is more efficient and stable than the G-level method (Youn et al. 2004a). However, the MPP-based method requires the first-order sensitivities of system responses. Moreover, it could generate relatively large error for highly nonlinear responses, such as responses with multiple MPPs.

The approximate integration method is a direct approach to estimate the probability density function (PDF; or statistical moments) through numerical integration. Numerical integration can be done in the input domain (Rahman and Xu 2004; Seo and Kwak 2003) or the output domain (Youn et al. 2005). Recently, the dimension reduction (DR) method (Rahman and Xu 2004; Xu and Rahman 2004) has been proposed and is known to be a derivative-free method. In the univariate DR method (Rahman and Xu 2004), it uses an additive decomposition of the responses that simplifies one multidimensional integration to multiple one-dimensional integrations. Generally, it provides accurate lower moments of system responses such as mean and SD. However, it may produce a relatively large error for higher moments of nonlinear system responses. Otherwise, it could be expensive with a large number of numerical integration points. In the general DR method (Xu and Rahman 2004), the theoretical error of the univariate DR method can be reduced by considering multivariate integrations. However, the computation effort increases significantly. Recently, the eigenvector dimension-reduction (EDR) method

(Youn et al. 2008) has been proposed to enhance the univariate DR method. The EDR method has three technical elements: (1) eigenvector sampling, (2) one-dimensional response approximations for effective numerical integration, and (3) a stabilized Pearson system. It has been found that the EDR method significantly improves numerical accuracy, efficiency, and stability in conducting a probability analysis for reliability and quality assessment. Moreover, the EDR method is capable of handling problems with non-normal distribution and statistical correlation as long as such information is disclosed.

This paper proposes a very efficient and accurate approach for reliability-based robust design optimization (RBRDO) by incorporating the EDR method. Even if the EDR method requires no sensitivity of the responses, RBRDO still requires sensitivity of reliability and quality to find a design direction in design optimization. In the proposed RBRDO method, an approximate response surface is exploited to calculate sensitivity of reliability and quality where the response surface is constructed using the eigenvector samples. Thus, sensitivity analysis becomes very efficient and simple. Three case studies (side impact crash, layered plate bonding process, and A-Arm in HMMWV) are used to demonstrate the effectiveness of the proposed RBRDO method using the EDR method.

2 Eigenvector dimension-reduction method

In general, the statistical moments of system responses can be calculated as

$$\mathbf{E}\left[Y^m\left(\mathbf{X}\right)\right] = \int_{-\infty}^{+\infty} \cdots \int_{-\infty}^{+\infty} Y^m\left(\mathbf{x}\right) \cdot f_{\mathbf{X}}\left(\mathbf{x}\right) \cdot \mathrm{d}x \qquad (1)$$

In (1), a major challenge is a multidimensional integration over the entire random input domain. To resolve this difficulty, the EDR method uses an additive decomposition from the univariate DR method (Rahman and Xu 2004) to convert a multidimensional integration in (1) into multiple one-dimensional integrations. Thus, (1) can be approximated as

$$\mathbf{E}\left[Y^m\left(\mathbf{X}\right)\right] \cong \mathbf{E}\left[\overline{Y}^m\left(\mathbf{X}\right)\right] = \int_{-\infty}^{\infty} \cdots \int_{-\infty}^{\infty} \bar{Y}^m \cdot f_{\mathbf{X}}\left(\mathbf{x}\right) \cdot \mathrm{d}x \qquad (2)$$

where $\overline{Y} = \Sigma_{j=1,N} Y\left(\mu_1, \ldots, \mu_{j-1}, X_j, \mu_{j+1}, \ldots, \mu_N\right) - (N-1) \cdot Y\left(\mu_1, \ldots, \mu_N\right)$. Using a binomial formula, (2) can be evaluated by executing one-dimensional integration recursively. Uncertainty of system responses can be evaluated through multiple one-dimensional

numerical integrations. However, there are still challenges to be addressed. For example, how to perform probability analysis with correlated random variables when the information of correlation is disclosed? How to predict the reliability from the statistical moments of a system response?

To address the challenges, the EDR method incorporates three technical components: (1) eigenvector sampling scheme (Section 2.1), (2) one-dimensional response approximations for effective numerical integration (Section 2.2), and (3) a stabilized Pearson system for PDF generation (Section 2.3).

2.1 Eigenvector sampling

Accuracy of probability analysis can be improved with an increase of the number of numerical integration points in (2). However, increasing the number of the integration points makes reliability-based robust design optimization (RBRDO) prohibitively expensive because responses at the points must be evaluated through simulation or experiment. To achieve both accuracy and efficiency in probability analysis, one-dimensional response surface will be created using samples along the eigenvectors of a random system (Section 2.2). The primary reason to choose samples along the eigenvectors is that the eigenvectors and eigenvalues contain information for statistical correlation and variation. So, the eigenvectors and eigenvalues assist finding samples over the random space. For efficiency, the EDR method employs only either three or five samples along each eigenvector (including a design point), depending on the nonlinearity of system responses. For N number of random variables, the EDR method demands $2N + 1$ or $4N + 1$ samples including the design point.

To obtain the eigenvectors and eigenvalues, an eigen-problem can be formulated as

$$\Sigma \mathbf{X} = \lambda \mathbf{X} \tag{3}$$

where $\mathbf{X}$ and λ are eigenvectors and eigenvalues of the covariance matrix, Σ. The covariance matrix with the N random input variables is defined as

$$\Sigma = \begin{bmatrix} \Sigma_{11} & \Sigma_{12} & \Sigma_{13} & \cdots & \Sigma_{1N} \\ \Sigma_{21} & \Sigma_{22} & \Sigma_{23} & \cdots & \Sigma_{2N} \\ \Sigma_{31} & \Sigma_{32} & \Sigma_{33} & \cdots & \Sigma_{3N} \\ \vdots & \vdots & \vdots & \ddots & \vdots \\ \Sigma_{N1} & \Sigma_{N2} & \Sigma_{N3} & \cdots & \Sigma_{NN} \end{bmatrix} = \begin{bmatrix} \sigma_1^2 & \Sigma_{12} & \Sigma_{13} & \cdots & \Sigma_{1N} \\ \Sigma_{21} & \sigma_2^2 & \Sigma_{23} & \cdots & \Sigma_{2N} \\ \Sigma_{31} & \Sigma_{32} & \sigma_3^2 & \cdots & \Sigma_{3N} \\ \vdots & \vdots & \vdots & \ddots & \vdots \\ \Sigma_{N1} & \Sigma_{N2} & \Sigma_{N3} & \cdots & \sigma_N^2 \end{bmatrix}$$

where the covariance between input variables X_i and X_j can be defined as

$$\text{Cov}(X_i, X_j) = \Sigma_{ij} = E\left[(X_i - \mu_i)(X_j - \mu_j)\right]$$

where μ_i and μ_j are the means of X_i and X_j. According to the definition, the covariance is symmetric with $\Sigma_{ij} = \Sigma_{ji}$ and σ_i^2 is the variance of any random variable X_i. Depending on statistical configuration of the system, four different types of problems can be defined: (a) uncorrelated and symmetric, (b) correlated and symmetric, (c) uncorrelated and asymmetric, and (d) correlated and asymmetric. For any circumstance, eigenvector samples will be found at

$$^1\mathbf{V}_i = \boldsymbol{\mu} - k\sqrt{\lambda_i}\mathbf{X}_i' \text{ and } ^2\mathbf{V}_i = \boldsymbol{\mu} + k\sqrt{\lambda_i}\mathbf{X}_i' \tag{4}$$

where $\mathbf{X}_i'$ and λ_i are the ith eigenvector and eigenvalue. The value of k determines the locations of the eigenvector samples along each eigen direction (say, $^1\mathbf{V}_i$) and the accuracy of one-dimensional response approximation. Subsequently, the response accuracy determines accuracy of one-dimensional numerical integrations and the EDR method. On the one hand, if the k is too large, accuracy of approximate one-dimensional response will be degraded on the inner side of eigenvector samples; on the other hand, if k is too small, accuracy of the response will be descended on the outer side of eigenvector samples because of the extrapolation. It is true that the accuracy of the EDR method becomes maximized with the optimal k value. However, it is nearly impossible to determine the optimal k analytically because of involvement of the response surface approximation (see Section 2.2). Thus, a parametric study that adjusts the k value from 1 to 6 for several numerical examples found two facts: (1) the accuracy of the EDR method appears to be the best with $k = [2.5\sim3.5]$; (2) the accuracy is nearly insensitive with any k value in the range. So, this paper uses $k = 3$ for eigenvector sampling. The eigenvector samples for the different types of problems are found as follows:

a. Uncorrelated and symmetric

If all random variables are statistically uncorrelated, all off-diagonal terms in the covariance matrix become zero. In this case, the eigenvectors are simply the original random variable axes. The eigenvector samples are obtained along the original random vectors at $^1\mathbf{V}_i = \boldsymbol{\mu} - 3\sqrt{\lambda_i}\mathbf{X}_i' = \boldsymbol{\mu} - 3\sigma_i\mathbf{X}_i'$ and $^2\mathbf{V}_i = \boldsymbol{\mu} + 3\sqrt{\lambda_i}\mathbf{X}_i' = \boldsymbol{\mu} + 3\sigma_i\mathbf{X}_i'$, where $\mathbf{X}_i'$ is the ith eigenvector where all elements are zero except the ith element is one.

b.   Correlated and symmetric

If some random variables are statistically correlated, the eigenvector samples are obtained at $^1\mathbf{V}_i = \mu - 3\sqrt{\lambda_i}\mathbf{X}_i'$ and $^2\mathbf{V}_i = \mu + 3\sqrt{\lambda_i}\mathbf{X}_i'$ along the eigenvectors of the eigenvalue problem in (3).

c.   Uncorrelated and asymmetric

If all random variables are statistically uncorrelated but asymmetrically distributed, the eigenvectors are still the same as the original random variable axes. To facilitate the eigenvector sampling for asymmetrically distributed random input parameters, the random parameters are transformed into standard-normally distributed random parameters (U), such as $\mathrm{T}: \mathbf{X}_i \rightarrow \mathbf{U}_i$. The eigenvector samples are similarly obtained along the eigenvectors in the transformed space at $^1\mathbf{U}_i = -3\mathbf{U}_i'$ and $^2\mathbf{U}_i = +3\mathbf{U}_i'$, where $\mathbf{U}_i'$ is the ith eigenvector where all elements are zero except the ith element is one. Then, two eigenvector samples $^1\mathbf{V}_i$ and $^2\mathbf{V}_i$ will be found from $^1\mathbf{U}_i$ and $^2\mathbf{U}_i$ through the inverse transformation, T^{-1}.

d.   Correlated and asymmetric

If some random variables are both correlated and with asymmetric distributions, the random parameters are first transformed into standard-normally distributed random parameters (**U**), such as $\mathrm{T}: \mathbf{X}_i \rightarrow \mathbf{U}_i$. After identifying the eigenvector in **U**-space, the scheme used for uncorrelated and asymmetric distributions will locate the eigenvector samples along the eigenvectors. Then, the samples in **X**-space will be obtained through an inverse transformation, as shown in Fig. 1d, so the responses at the samples can be calculated in the original **X**-space.

The $2N + 1$ eigenvector samples are illustrated for the four different cases shown in Fig. 1, and the samples are used for constructing one-dimensional response approximation using the SMLS method in the following section. To enhance numerical accuracy in probability analysis, the $4N + 1$ eigenvector samples will be selected with two extra samples located at $^3\mathbf{V}_i = \mu - 1.5\sqrt{\lambda_i}\mathbf{X}_i'$ and $^4\mathbf{V}_i = \mu + 1.5\sqrt{\lambda_i}\mathbf{X}_i'$.

Fig. 1 Eigenvector samples for the EDR method. **a** Symmetric and uncorrelated, **b** Symmetric and correlated, **c** Asymmetric and uncorrelated, **d** Asymmetric and correlated
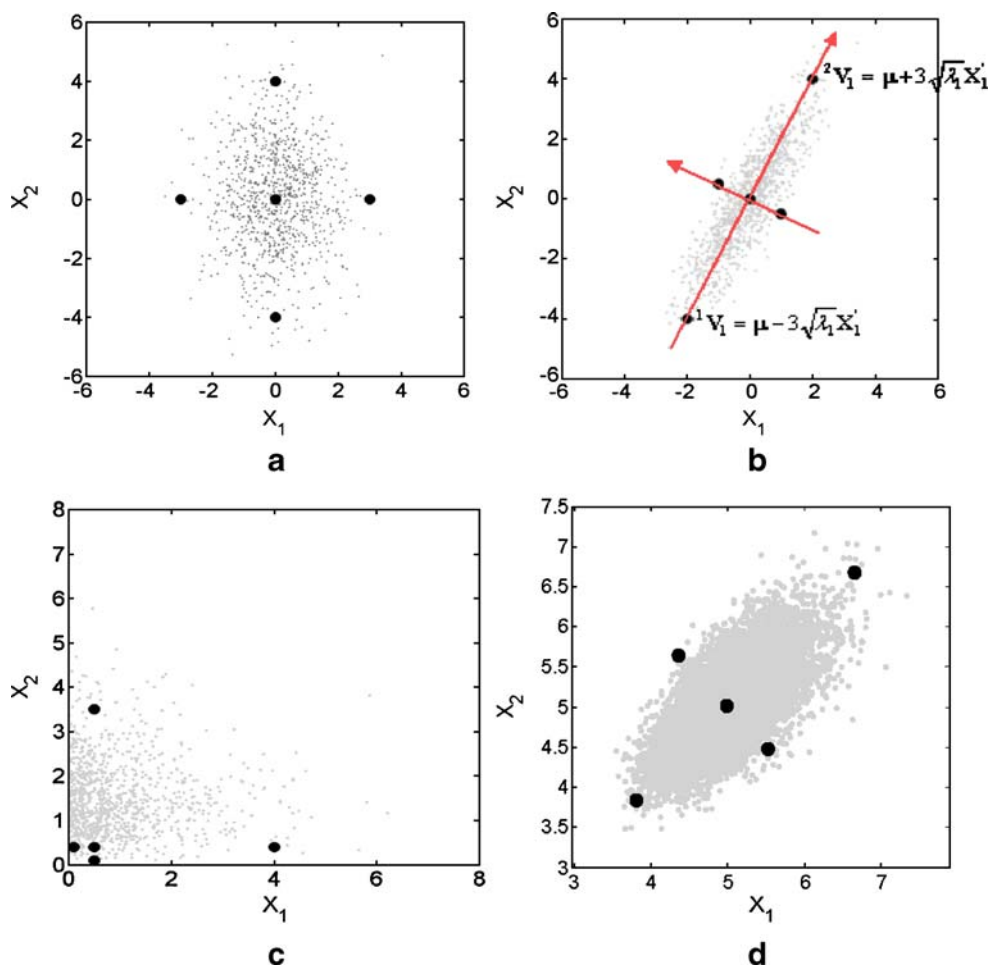
Table 1 PDFs of Pearson system (Johnson et al. 1995)

Type	Criteria	PDF
Normal	$c_1 = c_2 = 0$	$p(y) = K \exp\left[-(y+a)^2/(2c_0)\right],$ where $y \in (-\infty, \infty,)$
Types I and II	$c_1^2 - 4c_0 c_2 > 0$ and roots (a_1, a_2) of $c_0 + c_1 y + c_2 y^2 = 0$ satisfy $a_1 < 0 < a_2$	$p(y) = K(y-a_1)^{m_1}(a_2-y)^{m_2},$ where $m_1 = \dfrac{a+a_1}{c_2(a_2-a_1)}, m_2 = \dfrac{a+a_2}{c_2(a_1-a_2)}, y \in [a_1, a_2]$
Type III	$c_2 = 0, c_1 \neq 0$	$p(y) = K(c_0 + c_1 y)^m \exp\left(\frac{-y}{c_1}\right)$, where $m = c_1^{-1}\left(c_0 c_1^{-1} - a\right)$ If $c_1 > 0, y \in [-c_0/c_1, \infty)$; If $c_1 < 0, y \in (-\infty, -c_0/c_1]$
Type IV	$c_1^2 - 4c_0 c_2 < 0$	$p(y) = K\left[C_0 + c_2(y+C_1)^2\right]^{-(2c_2)^{-1}} \exp\left[-\dfrac{a-C_1}{\sqrt{c_2 C_0}}\tan^{-1}\dfrac{y+C_1}{\sqrt{C_0/c_2}}\right]$ where $C_0 = c_0 - c_1^2 c_2^{-1}/4, C_1 = c_1 c_2^{-1}/2, y \in (-\infty, \infty)$
Type V	$c_1^2 = 4c_0 c_2$	$p(y) = K(y+C_1)^{-1/c_2} \exp\left[\dfrac{a-C_1}{c_2(y+C_1)}\right]$, where $C_1 = c_1/(2c_2)$ If $(a-C_1)/c_2 < 0, y \in [-C_1, \infty)$; If $(a-C_1)/c_2 > 0, y \in (-\infty, -C_1]$
Type VI	Roots (a_1, a_2) of $c_0 + c_1 y + c_2 y^2 = 0$ are real and of the same sign	If $a_1 < a_2 < 0, p(y) = K(y-a_1)^{m_1}(y-a_2)^{m_2}$ where $y \in [a_2, \infty)$ If $a_1 > a_2 > 0, p(y) = K(a_1-y)^{m_1}(a_2-y)^{m_2}$ where $y \in (-\infty, a_2]$
Type VII	$c_1 = a = 0, c_0 > 0, c_2 > 0$	$p(y) = K\left(c_0 + c_2 y^2\right)^{-(2c_2)^{-1}}$, where $y \in (-\infty, \infty)$

2.2 Stepwise moving least squares method for numerical integration

For the calculation of statistical moments as shown in (2), multiple one-dimensional numerical integrations need to be performed recursively along the eigenvector directions as illustrated in Section 2.1. To enhance numerical efficiency and accuracy, approximate one-dimensional response surfaces will be constructed along the eigenvectors. So, the number of integration points can be increased as many as possible without extra computational cost. This section introduces the stepwise moving least square (SMLS) method for one-dimensional response approximation.

The moving least square (MLS) method (Youn and Choi 2004) is improved by a stepwise selection of basis functions, referred to as the stepwise moving least square (SMLS) method. The optimal set of basis terms is adaptively chosen to maximize numerical accuracy by screening the importance of basis terms. This technique is exploited for approximating the integrand in (2). The idea of the stepwise selection of basis functions comes from the stepwise regression method (Myers and Montgomery 1995; McAllister and Simpson 2003). The SMLS method for one-dimensional response approximation proceeds in the following steps:

Step 1. Define a pool of basis elements and default basis elements out of the pool. Set the total number of basis elements, *nb*, and sub-domain counter, *m* = 0. Prepare actual responses evaluated at the $2N + 1$ or $4N + 1$ eigenvector samples.
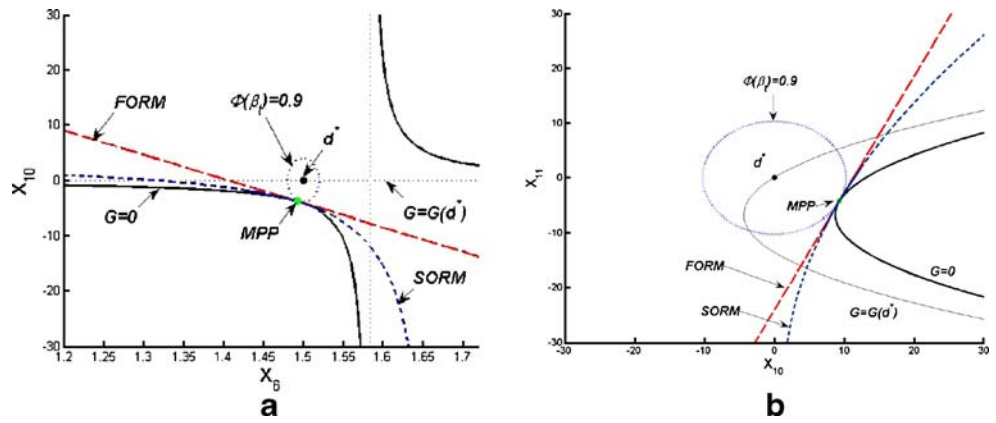
Step 2. Define the *m*th sub-domain surrounded by *nb* neighboring samples.

Step 3. Find *nt* training points in each sub-domain, where training points are defined in the middle of every two samples.
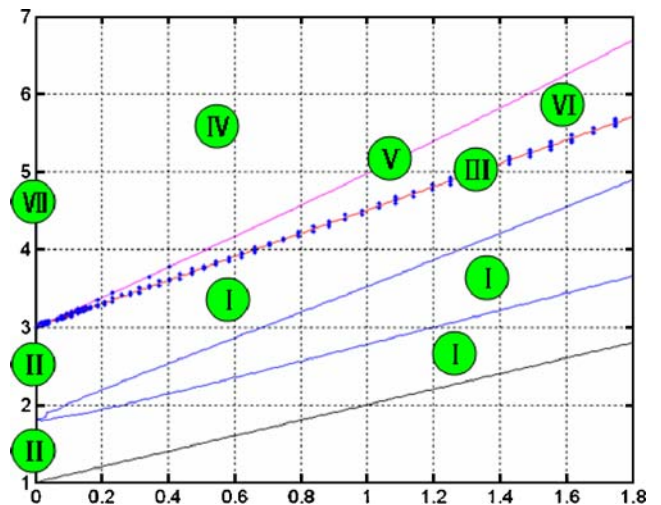
Fig. 2 Pearson curve (*x*-axis is the square of skewness, β_1, and *y*-axis is the kurtosis, β_2)

Fig. 3 FORM and SORM reliability analysis in hyper-plane for **a** G_8 and **b** G_{10}

Step 4. Approximate responses at training points using the MLS method as

$$\hat{\mathbf{Y}}\left(\mathbf{d}\right)=\mathbf{h}^{T}\left(\mathbf{d}\right)\mathbf{M}^{-1}\left(\mathbf{d}\right)\mathbf{B}\left(\mathbf{d}\right)\mathbf{Y} \;\; \text{where}\; \mathbf{M}=\mathbf{H}^{T}\mathbf{W}\left(\mathbf{d}\right)\mathbf{H},$$
$$\mathbf{B}=\mathbf{H}^{T}\mathbf{W}\left(\mathbf{d}\right)$$

where **W** is the weight matrix, **H** is the basis matrix, and **Y** is the actual responses at the eigenvector samples.

Step 5. Filter the basis elements adaptively in the mth sub-domains by ranking the magnitudes of the coefficients. The basis element with the maximum coefficient will be selected and added to the default basis elements. This process will be repeated until the total number of required basis elements (nb) is reached.

Step 6. Set $m = m + 1$ and go to Step 2 if $m \leq ns$ where ns is the total number of sub-domains. Otherwise go to Step 7.

Step 7. Construct one-dimensional response surface using sample responses.

Using actual responses evaluated at the $2N + 1$ or $4N + 1$ eigenvector samples, the SMLS method approximates the one-dimensional responses at all integration points. It is true that the increase of the number of numerical integration points enhances the accuracy of numerical integration and probability analysis. The use of the SMLS method can increase the integration points without extra simulations or experiments. Thus, in (2) a large number of integration points can be used to improve numerical accuracy in assessing statistical moments of the responses while maintaining high efficiency. The SMLS method can be integrated with any numerical integration methods, so the EDR method has no restriction to choose numerical integration schemes. The moment-based quadrature rule used in the DR method can be employed for the EDR method. However, a number of integration points must be predetermined before conducting the probability analysis. Even if the number of integration points is

Table 2 Results of component reliability analysis

Reliability of constraints	FORM	SORM	EDR	MCS
G_1	1	1	1	1
G_2	1	1	1	1
G_3	0.9989	0.9989	0.9989	0.9989
G_4	0.9000	0.9136	0.9026	0.9026
G_5	1	1	1	1
G_6	1	1	1	1
G_7	1	1	1	1
G_8	0.9000	0.8723	0.7097	0.7019
G_9	0.9897	0.9905	0.9905	0.9900
G_{10}	0.9000	0.9025	0.9495	0.9444
Function evaluation	47	47	23	100,000
Sensitivity evaluation	47	47	0	0
Hessian evaluation	0	10	0	0

increased for better accuracy, the information from the smaller number of integration points cannot be reused for that from the larger number. Besides, a large number of integration points may cause a numerical singularity of an inverse matrix for obtaining integration points. This paper also suggests an adaptive Simpson rule (Yamazaki and Shinozuka 1988) as an alternative integration method. Although the adaptive Simpson rule generally demands a larger number of integration points to preserve good accuracy compared to the moment-based quadrature rule, it gives more freedom on selection of probability distribution types for input random variables. Adaptive Simpson's rule adaptively identifies numerical integration points until the error of numerical integration is smaller than a user-specified tolerance.

2.3 A stabilized Pearson system

The EDR method calculates the first four statistical moments (mean, SD, skewness, and kurtosis) in (2). Then, the Pearson System (Johnson et al. 1995) is used to construct the PDF of a random response (Y) based on its first four moments. The detailed expression of the PDF can be achieved by solving a differential equation as
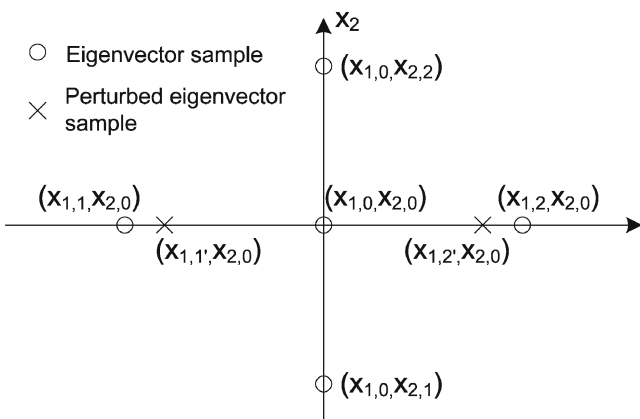
$$\frac{1}{p(Y)}\frac{dp(Y)}{dY} = -\frac{a+Y}{c_0 + c_1 Y + c_2 Y^2} \quad (5)$$

where a, c_0, c_1, and c_2 are four coefficients determined by the first four moments of the random response (Y) and expressed as
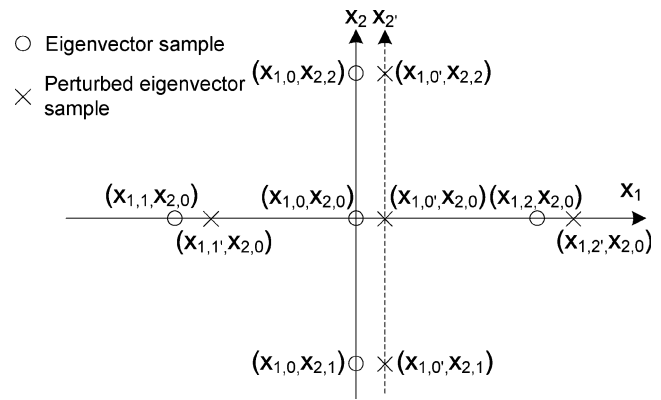
$$c_0 = (4\beta_2 - 3\beta_1)(10\beta_2 - 12\beta_1 - 18)^{-1}\mu_2$$
$$a = c_1 = \sqrt{\beta_1}(\beta_2 + 3)(10\beta_2 - 12\beta_1 - 18)^{-1}\sqrt{\mu_2}$$
$$c_2 = (2\beta_2 - 3\beta_1 - 6)(10\beta_2 - 12\beta_1 - 18)^{-1}$$

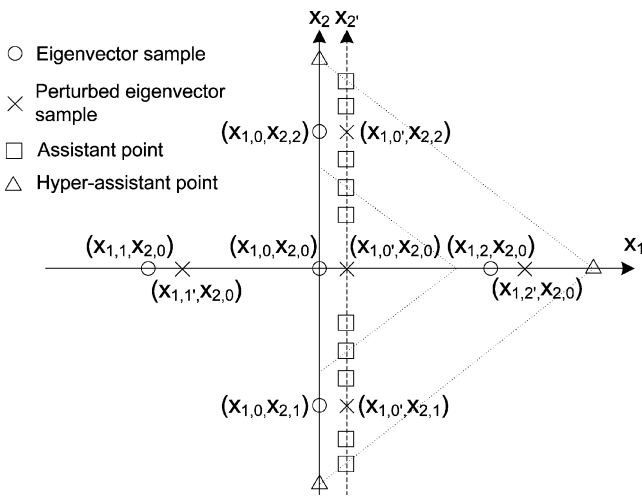**Fig. 4** Sensitivity with respect to a SD of the first random input ($2N + 1$ eigenvector sample scheme)

Fig. 5 Sensitivity with respect to a mean of the first random input ($2N + 1$ eigenvector sample scheme)

where β_1 is the squares of skewness, β_2 is the kurtosis, and μ_2 is the variation. The mean value is always treated as zero in the Pearson System, and it can be easily shifted to the true mean value once the differential equation is solved. The differential equation can be solved and its solutions, $p(Y)$, are classified into seven different distribution types, depending on the values of the four coefficients a, c_0, c_1, and c_2, as listed in Table 1. Normal distribution is a special case when $c_1 = c_2 = 0$. The coefficient K can be numerically calculated by forcing the integration of PDF in the defined domain to be a unity. The Pearson system, however, encounters a singularity problem while calculating the coefficient K at the solid dots as shown in Fig. 2.

In the EDR method, a stabilized Pearson system is proposed to avoid instability. In this system, the distribution at the singular point (skewness and kurtosis) in Fig. 2 is assumed to be a continuous function of the hyper-PDFs, where the hyper-PDFs must be selected as close to the distribution at the singular point as possible. The hyper-PDFs are obtained with positively and negatively perturbed kurtosis values rather than skewness because the hyper-PDFs with the kurtosis perturbation are much closer to the distributions than those with the skewness perturbation. Then these two hyper-PDFs are used to approximate the PDF at the singular point (or statistical moments) in Fig. 2.

Suppose that the Pearson system fails to construct a PDF with $[m_1, m_2, m_3, m_4]$. A detailed procedure follows:

Step 1. The first three moments are kept constant and gradually decrease the m_4 by a small decrement ($\Delta m_4 = 0.01$) until a PDF can be successfully constructed. $p_1(Y)$ and $m_{4,1}$ are denoted

Fig. 6 Sensitivity with respect to an input mean ($2N + 1$ integration scheme)

as the PDF and the corresponding kurtosis value, respectively.

Step 2. The first three moments are kept constant and gradually increase the m_4 by a small increment ($\Delta m_4 = 0.01$) until a PDF can be successfully constructed. $p_2(Y)$ and $m_{4,2}$ are denoted as the PDF and the corresponding kurtosis value, respectively.

Step 3. To build the PDF over the entire domain of the random response (Y), the response domain is discretized as Y_i, $i = 1$ to l. At every value Y_i, the PDF is obtained using two hyper-PDFs $p_1(Y_i)$ and $p_2(Y_i)$, where they are obtained with the kurtosis $m_{4,1}$ and $m_{4,2}$, respectively. With two hyper-PDF values having the kurtosis $m_{4,1}$ and $m_{4,2}$, the PDF $p(Y_i)$ with the actual kurtosis m_4 ($m_{4,1} < m_4 < m_{4,2}$) can be approximated using the SMLS method without a singularity. It is found that the PDF $p(Y_i)$ is accurately generated because the amount of the kurtosis perturbation is relatively small.

The perturbation size ($\Delta m_4 = 0.01$) of a kurtosis is used to preserve a relatively small perturbation. Basically, the smaller the difference between $m_{4,1}$ and $m_{4,2}$, the more accurate the PDF approximation for the actual kurtosis m_4.

3 Comparison of EDR, FORM, and SORM for reliability

In this example, the side impact crash model (Youn et al. 2004b) with multiple MPPs or high nonlinearity of responses (see Fig. 3) is employed to compare accuracy of the EDR method for reliability analysis with FORM and SORM. With 90% target reliability, RBDO using FORM produces the optimum design point at $[d*]^T =$ [0.500, 1.327, 0.500, 1.262, 0.623, 1.500, 0.500, 0.345, 0.192, 0.000, 0.000]^T. This optimum design is verified using four different methods: FORM, SORM, EDR, and MCS with 100,000 samples. The results are shown in Table 2. It is evident that the FORM produced large errors for reliability analysis compared with the MCS, especially for the constraints of G_8 and G_{10}. The SORM slightly reduces the error, but the EDR method predicts the reliability much more accurately.

The dashed and dotted lines show the first-/second-order approximations of failure surfaces used in the FORM and SORM for two active constraints of G_8 and G_{10} at the optimum design. Inaccurate approximations of failure surfaces lead to the significant errors in reliability values using the FORM and SORM, whereas the EDR method can precisely estimate the failure domains. Furthermore, as shown in Table 2, the EDR method is far more efficient than the other two, as the EDR method requires no sensitivity of system responses, and one EDR execution takes care of reliability analyses for a set of the crashworthiness constraints.

Table 3 Properties of design and random variables of vehicle side impact model

X_{10} and X_{11} are not design variable.

Random variables	Distr. Type	SD	d^L	d	d^U
X_1	Normal	0.050	0.500	1.000	1.500
X_2	Normal	0.050	0.500	1.000	1.500
X_3	Normal	0.050	0.500	1.000	1.500
X_4	Normal	0.050	0.500	1.000	1.500
X_5	Normal	0.050	0.500	1.000	1.500
X_6	Normal	0.050	0.500	1.000	1.500
X_7	Normal	0.050	0.500	1.000	1.500
X_8	Normal	0.006	0.192	0.300	0.345
X_9	Normal	0.006	0.192	0.300	0.345
X_{10}	Normal	10.0			
X_{11}	Normal	10.0			

Table 4 Components and safety rating criteria of vehicle side impact model

Components		Safety criteria
Objective: quality of abdomen load (kN)		≤ 1
$G_1 - G_3$: rib deflection	Upper	≤ 32
	Middle	
	Lower	
$G_4 - G_6$: VC (m/s)	Upper	≤ 0.32
	Middle	
	Lower	
G_7: Pubic symphysis force (kN)		≤ 4
G_8: Velocity of B-pillar		≤ 9.9
G_9: Velocity of front door at B-pillar		≤ 15.7

4 Probabilistic sensitivity analysis

At a given design point, sensitivity of quality and reliabilities with respect to a mean and a SD (or variation) of a random input must be provided to perform RBRDO. This is referred to as a probabilistic sensitivity analysis. Sensitivity of quality and reliabilities require sensitivity analysis of system responses (e.g., fatigue, stress, etc.) at the eigenvector samples. The sensitivity results at the samples are obtained using the finite difference method (FDM). Perturbation of mean or SD of a random input identifies new eigenvector samples. Then, the SMLS method is used to approximate the responses at the new eigenvector samples. Finally, the EDR method is performed to compute the perturbed quality and reliabilities with the perturbed mean or SD of the random input. Using the original and perturbed values of quality and reliabilities, the FDM computes sensitivities of quality or reliabilities.

4.1 Probabilistic sensitivity with respect to an input SD

This section considers a probabilistic sensitivity analysis with respect to a SD of a random input. As shown in Fig. 4, the new eigenvector sample points, $(x_{1,1'}, x_{2,0})$ and $(x_{1,2'}, x_{2,0})$, are identified with a perturbed SD of the random input, X_1. A perturbation size of 0.1% is commonly used for the FDM. For $x_{i,j}$, the first subscript (i) indicates the ith random parameter, and the second (j) indicates the jth sample point along each random parameter.

Table 5 Design history (case 1)

Iteration	0	1	2	3	4	Optimum
Number of analyses	230	230	230	230	230	1,150
Objective	0.693	0.158	0.130	0.114	0.114	0.114
Mean	0.643	0.117	0.090	0.073	0.073	0.073
SD	0.049	0.040	0.041	0.041	0.041	0.041
X_1	1.000	1.003	1.007	1.073	1.073	1.073
X_2	1.000	1.500	1.500	1.500	1.500	1.500
X_3	1.000	1.257	1.402	1.500	1.500	1.500
X_4	1.000	1.494	1.500	1.500	1.500	1.500
X_5	1.000	1.000	1.000	1.000	1.000	1.000
X_6	1.000	1.028	1.035	1.062	1.056	1.056
X_7	1.000	1.000	1.000	1.000	1.000	1.000
X_8	0.300	0.308	0.344	0.345	0.345	0.345
X_9	0.300	0.345	0.345	0.345	0.345	0.345
G_1	−0.018	−0.377	−0.102	−0.088	−0.101	Inactive
G_2	0.459	−2.762	−3.014	−3.237	−3.237	Inactive
G_3	4.295	0.015	0.001	0.000	0.000	Active
G_4	−0.079	−0.090	−0.093	−0.097	−0.097	Inactive
G_5	−0.095	−0.093	−0.089	−0.089	−0.089	Inactive
G_6	−0.035	−0.055	−0.065	−0.067	−0.067	Inactive
G_7	0.247	−0.065	−0.108	−0.142	−0.141	Inactive
G_8	0.313	−0.441	−0.459	−0.448	−0.453	Inactive
G_9	−0.157	−0.228	−0.302	−0.370	−0.365	Inactive

The SMLS method is used to approximate the response values at the two new eigenvector sample points when the $2N + 1$ eigenvector sample points are employed. Finally, the EDR method is performed to compute the quality (Q) and reliabilities (R_i) with the perturbed SD of the random input. The sensitivities of quality and reliabilities with respect to the SD of the ith random variable ($i = 1,..., N$) are computed using the following equations.

$$\frac{\partial Q}{\partial \sigma_{X_i}} \approx \frac{Q\left(\sigma_{X_i} + \Delta\sigma_{X_i}\right) - Q\left(\sigma_{X_i}\right)}{\Delta\sigma_{X_i}}$$

$$\frac{\partial R_k}{\partial \sigma_{X_i}} \approx \frac{R_k\left(\sigma_{X_i} + \Delta\sigma_{X_i}\right) - R_k\left(\sigma_{X_i}\right)}{\Delta\sigma_{X_i}} \text{ for } k = 1, \cdots, \text{NC}$$

(6)

where NC is the number of constraints for system responses.

4.2 Probabilistic sensitivity with respect to an input mean

This section considers a probabilistic sensitivity analysis with respect to a mean of a random input. The eigenvector samples with a perturbed mean of the random input are identified with a common perturbation size of 0.1%. The five new eigenvector samples with the perturbed mean of X_1 are identified at $(x_{1,0'}, x_{2,0})$, $(x_{1,1'}, x_{2,0})$, and $(x_{1,2'}, x_{2,0})$ along X_1 and $(x_{1,0'}, x_{2,1})$ and $(x_{1,0'}, x_{2,2})$ along $X_{2'}$, as shown in Fig. 5. The SMLS method

is used to approximate the responses at the five new eigenvector sample points when the $2N + 1$ eigenvector sample points are employed. Finally, the EDR method is performed to compute the quality (Q) and reliabilities (R_i) with the perturbed mean of the random input. The sensitivities of quality and reliabilities with respect to the mean of the ith random variable ($i = 1,..., N$) are computed using the following equations.

$$\frac{\partial Q}{\partial \mu_{X_i}} \approx \frac{Q\left(\mu_{X_i} + \Delta\mu_{X_i}\right) - Q\left(\mu_{X_i}\right)}{\Delta\mu_{X_i}}$$

$$\frac{\partial R_k}{\partial \mu_{X_i}} \approx \frac{R_k\left(\mu_{X_i} + \Delta\mu_{X_i}\right) - R_k\left(\mu_{X_i}\right)}{\Delta\mu_{X_i}} \text{ for } k = 1, \cdots, \text{NC}$$

(7)

The response values can be accurately approximated at the perturbed eigenvector samples located along X_1 axis, as the SMLS method accurately approximates the one-dimensional response along X_1, as illustrated in the Section 2.2. However, it is difficult to approximate the response values at the samples, $(x_{1,0'}, x_{2,1})$ and $(x_{1,0'}, x_{2,2})$, located along the axes other than $X_{1'}$. These samples and response values are referred to as the off-axis samples and response values. A feasible approach to resolve the difficulty is to approximate the off-axis response values using the assistant points (square), as shown in Fig. 6. The off-axis response values can be approximated using the SMLS method after the response values at the assistant points are obtained. In

Table 6 Design history (case 2)

Iteration	0	1	2	3	4	Optimum
Number of analyses	23	23	23	23	23	
Objective	0.693	0.296	0.140	0.115	0.115	0.115
Mean	0.643	0.258	0.099	0.073	0.073	0.073
SD	0.049	0.038	0.041	0.042	0.042	0.042
X_1	1.000	1.009	1.008	1.050	1.074	1.074
X_2	1.000	1.394	1.500	1.500	1.500	1.500
X_3	1.000	1.145	1.346	1.500	1.500	1.500
X_4	1.000	1.372	1.500	1.500	1.500	1.500
X_5	1.000	1.000	1.000	1.000	1.000	1.000
X_6	1.000	1.000	0.988	0.960	0.949	0.949
X_7	1.000	1.000	1.003	1.013	0.995	0.995
X_8	0.300	0.328	0.285	0.317	0.345	0.345
X_9	0.300	0.345	0.345	0.345	0.345	0.345
G_1	−0.018	−0.621	0.012	0.005	−0.334	Inactive
G_2	0.459	−2.593	−2.110	−2.592	−3.221	Inactive
G_3	4.295	0.446	0.576	0.476	−0.001	Active
G_4	−0.079	−0.092	−0.086	−0.094	−0.100	Inactive
G_5	−0.095	−0.098	−0.089	−0.088	−0.092	Inactive
G_6	−0.035	−0.063	−0.051	−0.061	−0.067	Inactive
G_7	0.247	0.022	−0.082	−0.119	−0.116	Inactive
G_8	0.313	−0.385	−0.362	−0.428	−0.540	Inactive
G_9	−0.157	−0.153	−0.240	−0.297	−0.275	Inactive

doing so, hyper-assistant points (triangle) are used to approximate the responses at the assistant points. The hyper-assistant points are defined along each variable axis (e.g., X_1, X_2) and their responses can be obtained with high accuracy. Along the dotted lines in Fig. 6, two hyper-assistant points are employed to approximate the response at one assistant point (square). It is found that the error in the response value could be relatively large when two hyper-assistant points are directly used for off-axis response approximation. Therefore, the responses at the assistant points are employed to approximate the responses at the perturbed eigenvector samples. Such an approach is expected to reduce a numerical error in probabilistic sensitivity estimation.

5 Reliability-based robust design optimization

Three practical engineering examples are used to show the effectiveness of the EDR method for RBRDO. To improve computational efficiency, RBRDO starts with $2N + 1$ and adaptively increases the sample size to $4N + 1$ if a response is known to be highly nonlinear.

5.1 Side impact crash problem

A vehicle side impact problem is considered for RBRDO with five different cases: (1) sensitivity calculation with actual function evaluation; (2) sensitivity

calculation with approximated function evaluation; (3) correlated random variables; (4) non-normal random variables; and (5) SD as the design parameter (Youn et al. 2004b). The sequential quadratic programming (SQP) is used in RBRDO for all five cases. All the design and random variables are shown in Table 3 for case 1 to case 3. In this example, the quality of the abdomen load is treated as an objective function with nine reliability constraints, as defined in Table 4. The quality is defined as the summation of mean and SD. The reliability level for all the constraints is set to 99.87%. The RBRDO is formulated as

$$\text{Minimize} \, Q = \mu_{\text{load}} + \sigma_{\text{load}}$$

$$\text{Subject to} \, R_k = P\left(G_k\left(X\right) \leq 0\right) \leq \Phi\left(-\beta_{t_k}\right),$$

$$k = 1, 2, \cdots, 9$$

$$0.5 \leq X_i \leq 1.5; \quad i = 1, \cdots, 7;$$

$$0.192 \leq X_i \leq 0.345; \quad i = 8, 9$$

where μ_{load} and σ_{load} are the mean and SD of abdomen load; $G_i(X)$ is the nine constraints defined in Table 4; and $\beta_{ti} = 3$.

Case 1 sensitivity calculation with actual function evaluation

The EDR method with $2N + 1$ eigenvector samples are employed to calculate the quality (objective

Table 7 Design history (case 3)

Iteration	0	1	2	3	4	5	Optimum
Number of analyses	23	23	23	23	23	23	
Objective	0.694	0.149	0.126	0.118	0.118	0.118	0.118
Mean	0.643	0.101	0.080	0.073	0.073	0.073	0.073
SD	0.051	0.048	0.046	0.045	0.044	0.044	0.044
X_1	1.000	1.008	1.046	1.073	1.099	1.101	1.101
X_2	1.000	1.500	1.500	1.500	1.500	1.500	1.500
X_3	1.000	1.331	1.459	1.500	1.500	1.500	1.500
X_4	1.000	1.500	1.500	1.500	1.500	1.500	1.500
X_5	1.000	1.000	0.999	0.998	0.998	0.998	0.998
X_6	1.000	1.176	1.129	1.091	1.043	1.040	1.040
X_7	1.000	1.000	1.006	1.008	1.009	1.009	1.009
X_8	0.300	0.325	0.345	0.345	0.337	0.336	0.336
X_9	0.300	0.345	0.345	0.345	0.345	0.345	0.345
G_1	−0.088	0.031	−0.001	−0.109	−0.318	−0.335	Inactive
G_2	0.380	−2.955	−3.259	−3.347	−3.388	−3.395	Inactive
G_3	4.295	0.021	−0.008	0.000	0.003	0.000	Active
G_4	−0.062	−0.070	−0.076	−0.079	−0.081	−0.082	Inactive
G_5	−0.090	−0.082	−0.081	−0.082	−0.085	−0.085	Inactive
G_6	−0.034	−0.060	−0.068	−0.069	−0.067	−0.067	Inactive
G_7	0.272	−0.034	−0.057	−0.058	−0.045	−0.044	Inactive
G_8	0.313	−0.332	−0.391	−0.425	−0.465	−0.468	Inactive
G_9	−0.282	−0.544	−0.570	−0.561	−0.523	−0.520	Inactive

Table 8 Properties of random input variables

Variable	Type	Mean	SD	Lower bound	Upper bound	Mode
X_1	Lognormal	1.000	0.050	–	–	–
X_2	Beta	1.000	0.050	0.500	1.300	–
X_3	Beta	1.000	0.050	0.500	1.300	–
X_4	Uniform	1.000	0.0866	–	–	–
X_5	Uniform	1.000	0.0866	–	–	–
X_6	Uniform	1.000	0.0866	–	–	–
X_7	Uniform	1.000	0.0866	–	–	–
X_8	Triangular	–	–	0.282	0.318	0.300
X_9	Triangular	–	–	0.282	0.318	0.300
X_{10}	Normal	0	10.000	–	–	–
X_{11}	Normal	0	10.000	–	–	–

function) and nine reliability constraints, respectively. For the sensitivity analysis of the quality and reliability, $(2N + 1)M$ function evaluations must be carried out, where N and M are the number of random and design variables, respectively. Although the computation is independent upon the number of the constraint and objective function, it is still expensive. The design history is shown in Table 5. In each iteration, $(2N+1)(M + 1)$ number of function evaluation is employed for the calculation of the quality, reliability constraints, and their sensitivity. After four design iterations, the optimum design is obtained where the third constraint becomes active and X_2, X_3, X_4, X_8 and X_9 reach their

upper bounds, as shown in Table 5. Using MCS with 100,000 random samples, the reliability of G_3 at the optimum design is found to be 99.87%.

Case 2 sensitivity calculation with approximated function evaluation

It is found that case 1 turns out to be very expensive (1,150 function evaluations). In case 2, sensitivity of the quality and reliability constraints are estimated using approximated responses. The design history is shown in Table 6 and the reliability of G_3 (active constraint) is confirmed as 99.87% at the optimum design using

Table 9 Design history (case 4)

Iteration	0	1	2	3	4	Optimum
Number of analyses	23	23	23	23	23	
Objective	0.699	0.216	0.156	0.135	0.135	0.135
Mean	0.643	0.159	0.096	0.073	0.073	0.073
SD	0.056	0.057	0.060	0.062	0.062	0.062
X_1	1.000	1.003	1.011	1.078	1.079	1.079
X_2	1.000	1.483	1.500	1.500	1.500	1.500
X_3	1.000	1.197	1.362	1.500	1.500	1.500
X_4	1.000	1.453	1.500	1.500	1.500	1.500
X_5	1.000	1.000	1.000	1.000	1.000	1.000
X_6	1.000	0.946	0.890	0.849	0.849	0.849
X_7	1.000	1.000	1.000	1.000	1.000	1.000
X_8	0.300	0.309	0.334	0.345	0.345	0.345
X_9	0.300	0.345	0.345	0.345	0.345	0.345
G_1	0.042	−0.679	−0.476	−0.537	−0.538	Inactive
G_2	0.507	−2.767	−2.923	−3.212	−3.213	Inactive
G_3	4.317	0.001	−0.003	−0.000	−0.000	Active
G_4	−0.079	−0.091	−0.095	−0.102	−0.102	Inactive
G_5	−0.094	−0.097	−0.094	−0.094	−0.094	Inactive
G_6	−0.036	−0.054	−0.060	−0.066	−0.066	Inactive
G_7	0.254	−0.437	−0.537	−0.587	−0.587	Inactive
G_8	0.314	−0.500	−0.573	−0.624	−0.624	Inactive
G_9	−0.062	−0.048	−0.080	−0.110	−0.110	Inactive

Table 10 Design history with standard deviation as the design parameter

Iteration	0	1	2	Optimum
Number of analyses	23	23	23	
Objective	0.116	0.086	0.085	0.085
Mean	0.073	0.073	0.073	0.073
SD	0.042	0.013	0.012	0.012
X_1	0.050	0.050	0.050	0.050
X_2	0.050	0.001	0.001	0.001
X_3	0.050	0.017	0.001	0.001
X_4	0.050	0.001	0.001	0.001
X_5	0.050	0.050	0.050	0.050
X_6	0.050	0.050	0.050	0.050
X_7	0.050	0.050	0.050	0.050
X_8	0.006	0.006	0.006	0.006
X_9	0.006	0.001	0.001	0.001
G_1	−0.334	−0.430	−0.435	Inactive
G_2	−3.221	−3.436	−3.438	Inactive
G_3	−0.001	−0.218	−0.218	Inactive
G_4	−0.100	−0.101	−0.101	Inactive
G_5	−0.092	−0.093	−0.093	Inactive
G_6	−0.067	−0.069	−0.069	Inactive
G_7	−0.116	−0.130	−0.130	Inactive
G_8	−0.540	−0.566	−0.566	Inactive
G_9	−0.275	−0.281	−0.282	Inactive

MCS with 100,000 samples. The optimum design in case 2 is slightly different from that in case 1 due to the approximate sensitivity. However, case 2 is far more efficient (150 function evaluations) than case 1 (1,150 function evaluations). FORM is also employed to carry out RBRDO, while the FDM is used for sensitivity computation. FORM requires a total of 1,734 function evaluations in RBRDO.

Case 3 correlated random variables

For correlated random variables, the EDR method identifies eigenvector samples, and then, the correlated problem is transformed to the uncorrelated. Then, the rest of the reliability analysis procedure is same as

case 2. In this example, x_2 and x_3, x_{10} and x_{11}, x_5 and x_7 are assumed correlated each other with the correlation coefficients as 0.7, 0.7, and -0.6, respectively. RBRDO converges to the optimum design at the five design iterations, as shown in Table 7. It is found that five design variables (X_1, X_5, X_6, X_7, X_8) are different at the optimum designs of cases 1 and 2. It indicates that the correlated random variables may have a significant impact to the reliability analysis and design. MCS with 100,000 samples verifies the reliability of G_3 as 99.88%.

Case 4 non-normal random variables

In this case, non-normal random variables are assumed to be dominated. These random inputs are listed

Fig. 7 Target bonding process and FE model. **a** Isometric view of the quarter model, **b** FM model
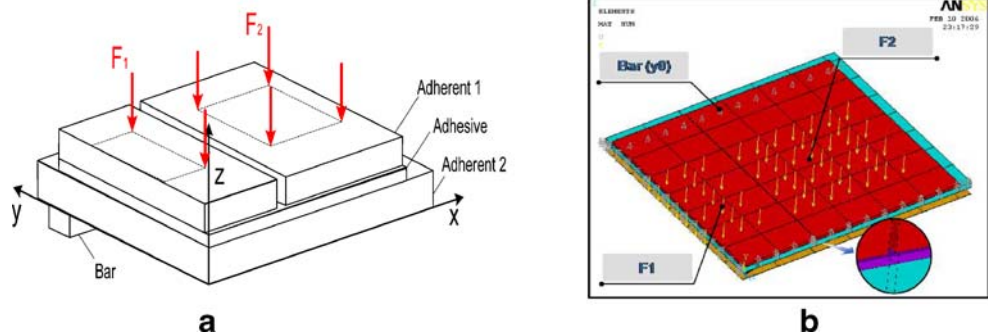
Table 11 Design/random properties of layered plate bonding model

Design variables	Distr. Type	Mean	SD
X_1	Normal	4,000	400
X_2	Normal	2,000	200
X_3	Normal	1	0.1

in Table 8. In the triangular distribution, the mode value is treated as design parameter unlike the mean value for all other distribution types. For the beta distribution with four parameters, the lower and upper bounds are assumed to be located at μ - 10σ and $\mu + 6\sigma$, respectively, where μ and σ indicate the mean and SD, respectively. For triangular distributions, both the lower and upper bounds are assumed to be 0.018 away from the mode value. After four design iterations, an optimum design is found with an active G_3 constraint as shown in Table 9. The optimum design is similar to that in case 2 except for a relatively larger SD of the objective function. The mean and SD of the objective function is confirmed as 0.073 and 0.064 by running MCS with 100,000 random samples. The reliability of G_3 is also confirmed as 99.87%.

Case 5 standard deviation as the design parameter

Generally, the mean of a random variable is regarded as a design parameter instead of the SD because it is difficult to control the SD rather than the mean value. Robust design attempts to minimize the SD of the objective function. In this case study, the optimum design in case 2 is defined as the initial design. Therefore, the contribution of the SDs of the random input variables to RBRDO results can be solely investigated. The sensitivity of quality and reliability is approximated using the approach stated in Section 4.1. The lower bound of the SD (x_1 to x_9) is set as 0.001, and noise variables (x_{10} and x_{11}) are non-designable. After two

design iterations, the SD of the objective function is reduced from 0.042 to 0.012 as the SD of design variables x_2, x_3, x_4, and x_9 are reduced to the lower bound 0.001 as shown in Table 10.

5.2 Robust design of layered bonding plates model

The bonding process of layered plates is very popular in the manufacturing of semiconductor or electronic display components. During this process, two-layered plates are bonded together by a suitable adhesive to form laminated stacks, which can be further processed in the following four steps:

1) heating the two plates above the melting temperature of the adhesive;
2) applying the adhesive at each surface of the plate;
3) putting them in contact with each other;
4) cooling them down to a room temperature.

In this process, residual stress due to the mismatch of the thermal expansion coefficients of two-layered plates could result in failures of the component such as crack, distortion, and interfacial delamination. Therefore, it is very important to accurately estimate the stress to improve the product quality. Herein, a transient thermal finite element (FE) analysis is used to predict the stress and deformation of plates. The model for the layered bonding plates is shown in Fig. 7. Considering the symmetry of the problem, a quarter of the model is used, as shown in Fig. 7a. Due to the brittle property and high stress at adherent 1, cracks and distortion

Table 12 Design history of layered bonding plates model

Iteration	Obj	Mean	SD	X_1	X_2	X_3	G_1	G_2	Number of analysis
0	23.322	23.020	0.302	4,000.000	2,000.000	1.000	−94.876	1.051	7
1	21.437	21.350	0.087	4,579.841	3,633.035	2.317	−85.742	0.108	7
2	21.358	21.215	0.143	4,659.514	4,704.467	3.356	−79.354	−0.467	7
3	21.177	21.040	0.137	4,316.124	5,000.000	3.734	−77.240	−0.631	7
4 ($2N+1$)	20.884	20.808	0.075	3,121.245	5,000.000	3.772	−77.371	−0.567	7
4 ($4N+1$)	20.976	20.862	0.115	3,121.245	5,000.000	3.772	−77.342	−0.563	6
5	20.909	20.802	0.110	2,752.275	4,996.178	3.024	−80.775	−0.207	13
6	20.900	20.798	0.102	2,554.780	4,998.089	2.862	−81.861	−0.122	13
7	20.898	20.795	0.103	2,520.106	4,998.208	2.849	−82.046	−0.114	13
Optimum	20.898	20.795	0.103	2,520.106	4,998.208	2.849	Inactive	Inactive	80
MCS	20.891	20.786	0.105	2,520.106	4,998.208	2.849	Inactive	Inactive	1.000

Fig. 8 Three loading variables (random variables). **a** Load variables (random variables), **b** Thickness variables (design variables)
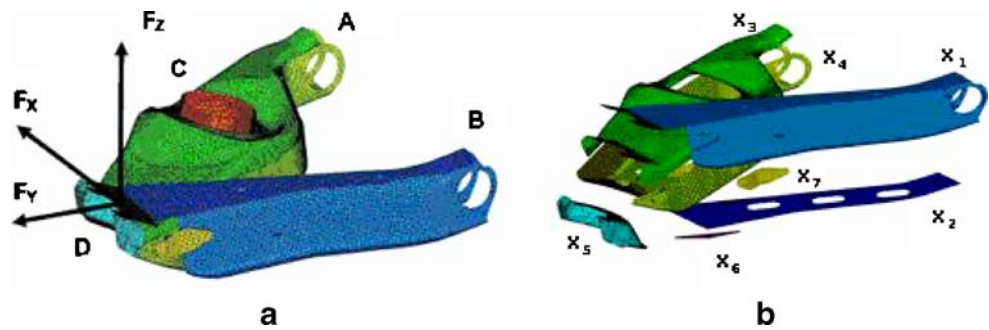
could occur. To reduce such defects, weights are applied on top of adherent 1, as shown in Fig. 7a, from the beginning of the process, and are removed at the end of the cooling process. The bonded assembly is placed on a pair of supporting bars, as shown in Fig. 7a. Three design variables, weight at the edge (X_1 or F_2), weight at the center (X_2 or F_1), and height of the bar (X_3 or y_0), are considered in this problem. Their statistical information is shown in Table 11. The objective function is to minimize the quality (summation of mean and SD) of residual stress. Two constraints are maximum stress during the process (<130 MPa) and center displacement (<3 mm).

The RBRDO is formulated as:

Minimize $\quad Q = \mu_r + \sigma_r$

Subject to $\quad R_i = P(G_i(X) \leq 0) \leq \Phi(-\beta_{t_i}), \quad i = 1, 2$

$\qquad 2,000 \leq X_1 \leq 10,000;$

$\qquad 1,000 \leq X_2 \leq 5,000; \quad 1 \leq X_3 \leq 5;$

where μ_r and σ_r are the mean and SD of residual stress; $G_1(X)$ is the instantaneous stress; $G_2(X)$ is the edge displacement; $\beta_{ti} = 3$.

The EDR method is applied to evaluate the quality (= mean + SD) of residual stress and the reliabilities of two constraints. As the responses are highly nonlinear, the SMLS method may produce inaccurate responses with only $2N + 1$ eigenvector samples. Subsequently, inaccurate responses may lead to inaccurate statistical moments of the system responses. To maximize numerical accuracy and efficiency in RBRDO, the sample size of the EDR method is adaptively decided. RBRDO starts with the $2N + 1$ sample size of the EDR method to efficiently reach the neighborhood of the optimum design and then continues with the $4N + 1$ sample size of the EDR method to achieve accuracy of the optimum design. The transition from $2N + 1$ to $4N+1$ is determined after satisfying a relaxed convergence criteria ($\varepsilon \leq 0.1$). This transition is found at the fourth design iteration in Table 12. Although the predicted

SD of the residual stress is 0.075 at the fourth design iteration, this value has relatively large error. It is confirmed by running the EDR with $4N + 1$ eigenvector samples at the same design. The SD is found to be 0.115 instead of 0.075. The SQP is used as a design optimizer in RBRDO. After eight design iterations, the optimum design is found where X_2 is close to the upper bound, as shown in Table 12. The EDR method requires totally 80 function evaluations for RBRDO. MCS with 1,000 random samples is used to confirm the EDR results at the optimum design. It is found that the results (the mean and SD of the residual stress) of the EDR method are very close to those of MCS at the optimum design. The overall quality is drastically improved by 38%.

5.3 Robust design of lower control A-Arm

Vehicle suspension systems experience intense loading conditions throughout their service lives. Control arms act as the backbone of suspension system, where the majority of these loads are transmitted through. Therefore, it is crucial that control arms be highly reliable, while minimizing its mass. For the purpose of demonstrating RBRDO using the EDR method, a HMMWV lower control arm is presented as a case study.

The lower control arm is modeled with plane stress elements using 54,666 nodes, 53,589 elements, and 327,961 DOFs, where all welds are modeled using rigid beam elements. For FE and design modeling, Hyper-Works 7.0 is used. The loading and boundary conditions for this case study are shown in Fig. 8a, where loading is applied at the ball-joint (point D) in three directions,

Table 13 Random properties of force for lower control A-Arm model

Random variable	Distribution
F_x	$\sim N(1,900, 95)$
F_y	$\sim N(95, 4.75)$
F_z	$\sim N(950, 47.5)$

**Table 14** Design variables in lower control A-arm model

Design variable	d_L	Initial des.	d_U	SD	Dist. Type
X_1	0.100	0.120	0.500	0.006	Normal
X_2	0.100	0.120	0.500	0.006	Normal
X_3	0.100	0.180	0.500	0.009	Normal
X_4	0.100	0.135	0.500	0.007	Normal
X_5	0.150	0.250	0.500	0.013	Normal
X_6	0.100	0.180	0.500	0.009	Normal
X_7	0.100	0.135	0.500	0.007	Normal

and the boundary conditions are applied to simulate the bushing joints (points A and B) and the joint with a shock absorber and spring assemble (point C). The design variables are the thicknesses of the seven major component of the control arm, as shown in Fig. 8b. The statistical information of these components is shown in Tables 13 and 14. The thicknesses are considered as random design variables, whereas the loading condition is considered as random noise variables.

To determine the hot spots (high stress concentrations) in the model, which are used to determine the constraints, a worst case scenario analysis of the control arm is performed. For this worst case scenario, all the design variables are set at their lower bounds, and all the loads are set at their high values. From the worst case scenario, 91 constraints (G_1 to G_{91}) are defined on several critical regions using the von Mises stress, as shown in Fig. 9. In this case study, the quality function (= mean + SD) of mass is treated as objective function and a target stress value for 91 stress constraints is set to 60.9 ksi. The reliability level for all the constraints is set to 99.87%.

The EDR method with $2N + 1$ (=21) FE analyses is carried out to evaluate the quality of the mass,

91 reliability constraints, and their sensitivities at any design iteration, where $N = 10$ (seven for random design parameters and three for random loads). The SQP is used for an optimizer in RBRDO. At initial design, the 6th and 80th constraints severely violate the required reliability. After seven design iterations, the optimum design is found where the aforementioned two and 87th constraints become active. The design variables X_1 and X_5 reach the lower bound, and X_6 reaches the upper bound, as shown in Table 15. The EDR method requires totally 147 FE simulations for RBRDO. In this example, even though RBRDO begins with the severely violated initial design, the mass is slightly increased because X_6 ensures high reliability of the stress with only a small increase in the overall mass unlike other design variables. MCS with 10,000 random samples is also employed to confirm the EDR results at optimum design. The mean and SD of mass are confirmed as 31.967 and 0.712. Using MCS, the reliabilities of the 6th, 80th, and 87th active constraints are confirmed as 99.84%, 99.86%, and 99.89%, respectively, and all other constraints are confirmed inactive. The stress comparison at initial and optimum designs for the 6th and 80th constraints is shown in Fig. 10.

Fig. 9 Ninety-one critical constraints of the lower control A-arm model
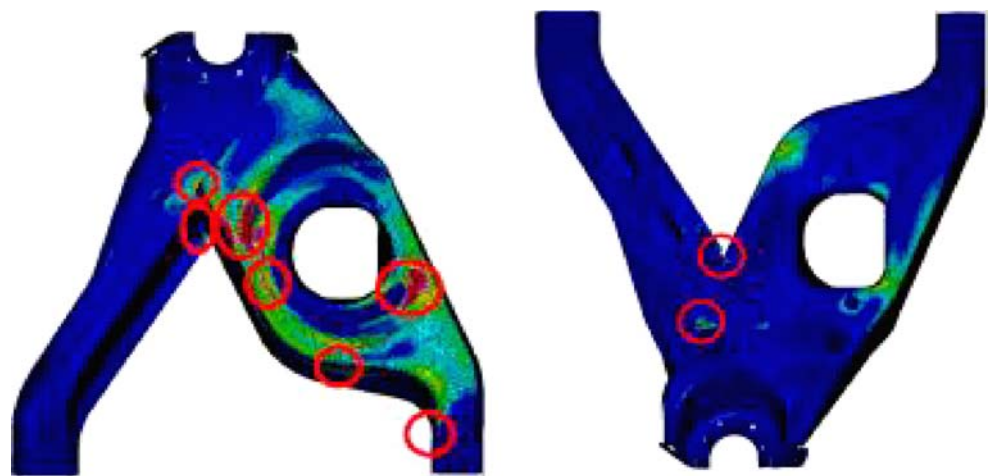
**Table 15** Design history of lower control A-arm model

Iteration	0	1	2	3	4	5	6	7	Opt.
Number of analyses	21	21	21	21	21	21	21	21	
Objective	31.474	32.011	32.694	32.644	32.680	32.683	32.680	32.680	32.680
Mean	30.762	31.299	31.982	31.931	31.968	31.971	31.967	31.968	31.968
SD	0.712	0.712	0.712	0.712	0.712	0.712	0.712	0.712	0.712
X_1	0.120	0.100	0.100	0.100	0.100	0.100	0.100	0.100	0.100
X_2	0.120	0.140	0.140	0.140	0.140	0.140	0.140	0.140	0.140
X_3	0.180	0.158	0.164	0.163	0.163	0.163	0.163	0.163	0.163
X_4	0.135	0.160	0.162	0.165	0.166	0.166	0.165	0.166	0.166
X_5	0.250	0.150	0.150	0.150	0.150	0.150	0.150	0.150	0.150
X_6	0.180	0.500	0.500	0.500	0.500	0.500	0.500	0.500	0.500
X_7	0.135	0.100	0.291	0.148	0.107	0.141	0.138	0.136	0.136
G_6	1.388	0.109	−0.006	0.003	0.000	0.000	0.000	0.000	Active
G_{80}	2.804	0.365	0.006	0.029	0.009	−0.004	0.001	0.000	Active
G_{87}	−0.490	0.262	−0.021	0.003	0.000	0.000	0.000	0.000	Active

6 Conclusion

This paper proposes an effective approach for RBRDO by incorporating the EDR method. It has been shown that the use of the EDR method provides three benefits to RBRDO. First, an approximate response surface facilitates sensitivity calculation of reliability and quality where the response surface is constructed using the eigenvector samples. Thus, sensitivity analysis becomes very efficient and simple. Second, one EDR execution evaluates a set of quality (objective) and reliability (constraint) functions. In general, the EDR requires $2N + 1$ or $4N + 1$ simulation runs where N is the total number of random variables. Unlike FORM or SORM, the EDR execution does not require an iterative process, so the proposed RBRDO methodology has a single-loop structure. Moreover, the EDR execution time can be much shorter by taking advantage of a parallel computing power, and RBRDO can be far more efficient. Third, the EDR method allows

Fig. 10 Stress comparison of initial and optimum design. **a** G_6 at initial design, **b** G_6 at optimum design, **c** G_{80} at initial design, **d** G_{80} at optimum design
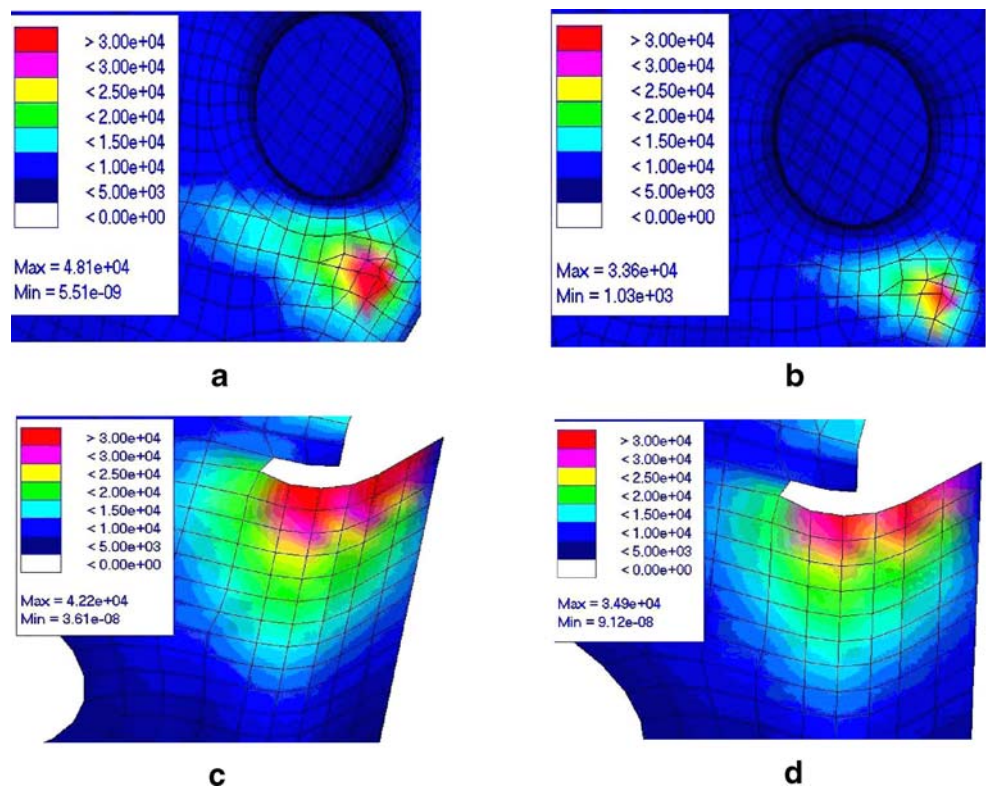
solving problems with statistical correlated and non-normally distributed random inputs. This study also found that the EDR method could be more accurate than FORM and SORM for the problems with multiple MPPs or highly nonlinear limit state functions. As demonstrated with three case studies (side impact crash, layered plate bonding process, and A-Arm in HMMWV), it is expected that the proposed RBRDO using the EDR method can enhance numerical efficiency substantially while maintaining good accuracy. Even though the EDR method provided many desirable features to RBRDO, the use of the EDR method must be carefully considered when system responses have high-order interaction terms or when high target reliability (e.g., greater than 99.9%) is required.

References

Bjerager P (1988) Probability integration by directional simulation. ASCE J Engng Mech 114:1285–1302

Bucher CG (1988) Adaptive sampling—an iterative fast Monte Carlo procedure. Struct Saf 5:119–126

Du X, Chen W (2002) Sequential optimization and reliability assessment method for efficient probabilistic design. DETC-DAC34127, ASME design engineering technical conferences, Montreal, Canada, September

Engelund S, Rackwitz R (1993) A benchmark study on importance sampling techniques in structural reliability. Struct Saf 12:255–276

Hasofer AM, Lind NC (1974) Exact and invariant second-moment code format. J Eng Mech ASCE 100:111–121

Johnson NL, Kotz S, Balakrishnan N (1995) Continuous univariate distributions. Wiley, New York

Jung DH, Lee BC (2002) Development of a simple and efficient method for robust optimization. Int J Numer Methods Eng 53:2201–2215

Kleiber M, Hien TD (1992) The stochastic finite element method. Wiley, New York, NY

Lin CY, Huang WH, Jeng MC, Doong JL (1997) Study of an assembly tolerance allocation model based on Monte Carlo simulation. J Mater Process Technol 70:9–16

McAllister CD, Simpson TW (2003) Multidisciplinary robust design optimization of an internal combustion engine. J Mech Des Trans ASME 125(2):124–130

Melchers RE (1989) Importance sampling in structural systems. Struct Saf 6:6–10

Myers HR, Montgomery DC (1995) Response surface methodology. Wiley, New York

Niederreiter H, Spanier J (2000) Monte Carlo and quasi-Monte Carlo methods. Springer, Berlin

Rahman S, Rao BN (2001) A perturbation method for stochastic meshless analysis in elastostatics. Int J Numer Methods Eng 50:1961–1991

Rahman S, Xu H (2004) A univariate dimension-reduction method for multi-dimensional integration in stochastic mechanics. Probab Eng Mech 19:393–408

Seo HS, Kwak BM (2003) An improved reliability analysis using design of experiments and an application to tolerance design. The 5th world congress of structural and multidisciplinary optimization, Lodo do Jesolo, Italy, May 19–23

Sobol IM (1998) On quasi-Monte Carlo integrations. Math Comput Simul 47:103–112

Varghese P, Braswell RN, Wang B, Zhang C (1996) Statistical tolerance analysis using FRPDF and numerical convolution. Comput-Aided Des 28(9):723–732

Wu Y-T (1994) Computational methods for efficient structural reliability and reliability sensitivity analysis. AIAA J 32(8):1717–1723

Xu H, Rahman S (2004) A generalized dimension-reduction method for multidimensional integration in stochastic mechanics. Int J Numer Methods Eng 61:1992–2019

Yamazaki F, Shinozuka M (1988) Neumann expansion for stochastic finite element analysis. J Eng Mech ASCE 114:1335–1354

Youn BD, Choi KK (2004) A new response surface methodology for reliability-based design optimization. Comput Struct 82:241–256

Youn BD, Choi KK, Du L (2004a) Adaptive probability analysis using an enhanced hybrid mean value (HMV+) method. J Struct Multidisc Optim 28(4):319–333

Youn BD, Choi KK, Gu L, Yangf R-J (2004b) Reliability-based design optimization for crashworthiness of side impact. J Struct Multidisc Optim 26(3–4):272–283

Youn BD, Choi KK, Yi K (2005) Performance moment integration for quality assessment in reliability-based robust design optimization. Mech Des Struct Mach 33:185–213

Youn BD, Xi Z, Wang PF (2008) Eigenvector dimension reduction (EDR) method for sensitivity-free probability quantification. Struct Multidisc Optim (in press)